RSC Advances

PAPER

View Article Online
View Journal | View Issue

Cite this: *RSC Adv.*, 2019, **9**, 20240

Broadband terahertz recognizing conformational characteristics of a significant neurotransmitter γ-aminobutyric acid†

Chao Cheng,[abc] Zhongjie Zhu,[ac] Shaoping Li,[b] Guanhua Ren,[acd] Jianbing Zhang,[ac] Haixia Cong,[c] Yan Peng,[e] Jiaguang Han,[d] Chao Chang*[f] and Hongwei Zhao *[ac]

γ-Aminobutyric acid (GABA) is the chief inhibitory neurotransmitter in the central nervous system, its conformational behavior is critical for selective biological functions and the process of signal transmission. Although this neuroactive molecule has been extensively studied, its vibrational properties related to the conformation and intermolecular interactions in the terahertz (THz) band have not been identified experimentally yet. In this study, we applied a broadband THz time-domain spectroscopy (THz-TDS) system from 0.5 to 18 THz to characterize a unique THz fingerprint of GABA. The density functional theory calculation results agree well with the THz experimental spectrum. The study shows that the vibrational modes of GABA at 1.15 and 1.39 THz originate from distinct collective vibrations. The absorptions at the higher THz frequencies also carry part of collective vibrations, but more reflect the specific and local vibrational information, including the skeleton deformation and the rocking of the functional groups, which are closely associated with the conformation and flexibility of GABA. This study may help to understand the conformational transitions of neurotransmitter molecules and the resonant response to THz waves.

Received 21st April 2019
Accepted 19th June 2019

DOI: 10.1039/c9ra02971k

rsc.li/rsc-advances

1 Introduction

γ-Aminobutyric acid (GABA) is an inhibitory neurotransmitter in the vertebrate central nervous system and plays a fundamental role in the balance between neuronal excitation and inhibition; the imbalance between excitation and inhibition can lead to coma, depression, convulsions, anxiety, restlessness, and insomnia.[1–4] GABA has modulatory effects on enteric neurons and immune cells. Changes in GABA metabolism may be associated with the origin and spread of seizure activity. Furthermore, the pharmaceutical use of GABA in the treatment of certain neurological disorders, such as Parkinson's disease and epilepsy, has also been reported.[2,5,6]

GABA has an amino group attached to the gamma carbon and a carboxyl group connected to the alpha carbon at the other end of the carbon chain. GABA molecules are zwitterions (with the amino group protonated and the carboxyl group deprotonated), partially folded, flexible, and held in a cross-linked chain arrangement by hydrogen bonds.[7] Two different conformations of GABA, *gauche* and *trans*, have been reported in previous work.[8,9] Besides, its molecular structure may help resolve its mode of action at some regions of the mammalian brain.[1,7] Therefore, the study of the conformation and structure of GABA may throw some light on the conformational preference for binding with the receptor and help understand the ability of GABA to activate receptors.[1,10]

Vibrational spectroscopies, including Fourier-transform infrared (FTIR) spectroscopy and Raman spectroscopy, can provide fundamental and useful information on molecular structure and conformation. Studies have shown that terahertz (THz) spectroscopy can be used to successfully distinguish polymorph pharmaceuticals, research the interactions of chemical materials, and quantitatively detect impurities in organic crystals.[11–13] Moreover, THz spectroscopy is sensitive to hydrogen bonding, lattice vibration, water of crystallization, and conformational change.[11,14] Hand *et al.*[15] revealed that THz spectroscopy between 1 and 10 THz can obtain more abundant low-frequency vibrational information of molecules, and THz spectra of many biomolecules between 6–9 THz corresponding to the densest transitions between states. Compare with the

[a]*Zhangjiang Laboratory, Shanghai Advanced Research Institute, Chinese Academy of Sciences, Shanghai 201210, China*
[b]*School of Chemical Engineering, East China University of Science and Technology, Shanghai 200237, China*
[c]*Shanghai Institute of Applied Physics, Chinese Academy of Sciences, Shanghai 201800, China. E-mail: zhaohongwei@sinap.ac.cn*
[d]*Center for Terahertz Waves and College of Precision Instrument and Optoelectronics Engineering, Key Laboratory of Optoelectronics Information and Technology, Ministry of Education, Tianjin University, Tianjin 300072, China*
[e]*Shanghai Key Lab of Modern Optical System, University of Shanghai for Science and Technology, No. 516, Jungong Road, Shanghai 200093, China*
[f]*Advanced Interdisciplinary Technology Research Center, National Innovation Institute of Defense Technology, Beijing 100071, China. E-mail: changc@xjtu.edu.cn*

† Electronic supplementary information (ESI) available. See DOI: 10.1039/c9ra02971k

THz systems equipped with solid state emitters and sensors, gases have no phonon resonances or echoes due to THz or optical reflections, enabling broadband THz spectroscopy free of instrumental artifacts.[16] Bartel *et al.*[17] generated single-cycle THz transients in the frequency range 0.3–7 THz by using a Ti:sapphire amplifier in ionized air. Dai *et al.*[18] reported the first demonstration of broadband THz wave detection through third-order nonlinear optical processes using gases as the sensor, and the wider spectral range of their improved system allows spectroscopic measurement across the full THz range and even enter the middle infrared.[16] The broadband THz response does not interfere with THz sensitivity to biomolecular binding and the universal THz binding sensitivity has application potential for biosensing.[19] Recently, Dampf *et al.*[20] studied temperature-dependent THz-TDS spectra from 10 to 135 cm^{-1} (1 THz ~33.33 cm^{-1}) of GABA, they found an anomalous frequency shift upon cooling and further explained it by the quasiharmonic approximation in solid-state density functional theory (DFT) simulations. da Silva *et al.*[2] investigated GABA in the range of 30 to 1700 cm^{-1} with Raman spectroscopy between 1 atm and 7.1 GPa, and they interpreted the modifications in the Raman spectra mainly on the basis of the conformational changes of the molecules in the unit cell. Du *et al.*[21] studied GABA, benzoic acid (BA), and the corresponding cocrystal by Raman spectroscopy in the range of 150 to 3250 cm^{-1} and THz spectroscopy from 0.2 to 1.7 THz. They found that the formation of a GABA-BA cocrystal under slow solvent evaporation is affected by the pH value of the aqueous solution. Peng *et al.*[22] researched two typical metabolites and three typical neurotransmitters, including GABA, from 0.9 to 4.5 THz by FTIR and successfully identified the components and proportions of a mixture consisting of neurotransmitters and neurotrophic substances. These works provide useful characteristics of GABA in the THz region and the tentative assignments of its modes. However, the details of the vibrational modes of GABA are still insufficient and the interpretation of the relationship between the THz signal and the biological function of the molecular vibration has not been clarified.

In this work, GABA was studied with an air-plasma based broadband THz time-domain spectroscopy (THz-TDS) system from 0.5 to 18 THz and was checked by another THz system (TAS7400TS) between 0.5 and 4.0 THz. To make out the difference of the above two systems at about 1 THz, an additional photoconductive-switch-based THz system, whose effective range is 0.2 to 2.5 THz, was used. The temperature effect on GABA from 83 to 363 K was investigated with the TAS7400TS fast scanning THz system. To better interpret the origin of the absorption peaks and corresponding vibrational modes of the experimental THz spectrum, the solid-state density functional theory calculation based on the crystal structure was performed. Considering GABA has polymorphism phenomenon, powder X-ray diffraction (PXRD) was utilized and the result indicated that the GABA we used belonged to the monoclinic system. A mid-infrared FTIR was also carried out to further check the broadband THz spectrum of GABA. The results demonstrate that the absorption of the broadband THz spectrum from 13 to 16 THz is mainly from the substrate and that the contribution of GABA is relatively small.

2 Materials and methods

2.1 Materials

GABA (≥98%) was purchased from J&K, cyclic olefin copolymer (COC) powder was obtained from the experimental plant of the Shanghai Institute of Nuclear Research (SINR), and KBr (≥99%) was obtained from Sinopharm Chemical Reagent Co., Ltd. COC was found to be suitable for THz spectrum applications because of its negligible refractive-index dispersion and negligible absorption in the THz band.[23] All the samples were used without further purification.

2.2 Sample preparation

GABA/COC at a mass ratio of 1 : 15–18 was gently ground into fine particles; the mixture was then compressed into a pellet (13 mm in diameter) with a hydraulic press at a pressure of 2 MPa.

2.3 Terahertz time-domain spectroscopy (THz-TDS)

The spectra between 0.5 and 18 THz were measured using a THz spectrometer based on air-plasma generation and detection with a resolution of 1.9 GHz. A Ti:sapphire amplified laser system (Spitfire ACE, Spectra-Physics) was used to emit ultrashort 800 nm laser pulses of ~35 fs duration at a 1 kHz repetition rate. The pulse energies used to generate the THz radiation and the detection were about 0.9 mJ and 80 μJ respectively. The voltage for the air-biased coherent detection was 1.5 kV. A TAS7400TS THz-TDS system (Advantest Corporation, Japan) based on the $LiNbO_3$ nonlinear optical crystal with 1560 nm wavelength, 300 fs pulse width, 1.9 GHz frequency resolution, and 0.5 to 4.0 THz effective range was used to check the broadband THz spectrum of GABA below 4.0 THz and for the variable temperature experiment. Because this system employs phase-modulation dual-laser synchronous control technology without a mechanical optical delay line, it enables fast scanning. Therefore, real-time dynamic data in the variable temperature process was obtained with this system. The THz absorption spectrum of GABA between 0.2 and 2.5 THz was measured using a photoconductive switch-based 8-F confocal THz-TDS system with a resolution of 1 GHz. A mode-locked Ti:sapphire laser (Spectra-Physics, USA), capable of generating 80 MHz, 800 nm, and 80 fs ultrafast optical pulses, was used as the light source to generate and detect THz waves. Fig. 1 shows a schematic diagram of the broadband air-plasma THz system.

Drying air was continuously pumped into the THz system to keep the relative humidity under 1.0% during the measurements. The spectrum of each sample was the average of three measurements with the drying air as reference. The measurements with the THz system based on the air-plasma and the system based on the photoconductive switch included 1024 scan numbers. In order to obtain the real-time dynamic data at

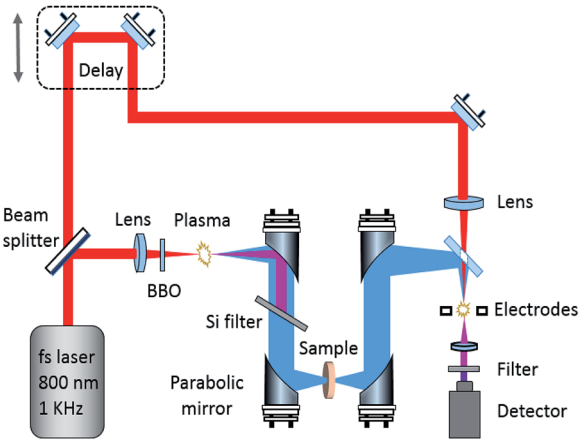

Fig. 1 Illustration of the broadband air-plasma THz system.

variable temperatures, 512 scan numbers were selected on the system based on the $LiNbO_3$ nonlinear optical crystal.

2.4 Temperature controller

The pellet of GABA was placed into a temperature controller (Specac Ltd. U.K., accuracy ± 0.5 °C) equipped with cyclic olefin copolymer windows. Liquid nitrogen was poured into the variable temperature cavity. A series of THz spectra of GABA were recorded from 83 to 363 K.

2.5 Powder X-ray diffraction (PXRD)

The PXRD pattern of GABA was measured using the Bruker D8 Advance (Cu source, 40 kV voltage, 40 mA filament emission). The data was collected with a scan from 10 to 90° (2θ).

2.6 Fourier transform infrared spectroscopy (FTIR)

A FTIR Nicolet Avatar 370 spectrometer (resolution 4 cm^{-1}) from 400 to 4000 cm^{-1} was used to check the spectrum of the sample obtained by the broadband air-plasma THz system. KBr was used as substrate for the experiment.

3 Quantum chemical calculation

Considering that THz spectrum is very sensitive to the crystalline forms, PXRD was carried out to confirm that GABA used in the experiments and theoretical calculation are the same crystalline form. Several crystallographic atomic coordinates of GABA were found in the published crystal databases.[7–9,24,25] The experimental PXRD pattern of GABA agreed very well with the calculated PXRD pattern using the crystal cell parameters from ref 8 (see ESI Fig. S1†) and the results demonstrated that the crystal structure of the GABA we used in the experiments was monoclinic. Therefore, the space group $P2_1/a$ ($Z = 4$), and a = 8.214 (2), b = 10.000 (2), c = 7.208 (2) Å, β = 110.59 (2)° were selected as the initial parameters for the calculation.[8]

The geometry optimization and energy calculations were carried out based on the solid-state DFT using the CASTEP[26] program, a part of the Materials Studio package from Accelrys. Grimme's dispersion-corrected method was chose before we conducted geometry optimization. The result was obtained for the crystalline state with the generalized gradient approximation (GGA)-Perdew–Burke–Ernzerhof (PBE) correlation functional.[27] Calculations were performed using a norm-conserving pseudopotential in CASTEP. The quality of the energy calculation was ultra-fine. The plane-wave cut-off energy was 830 eV. For GABA, Brillouin zone sampling of electronic states was performed on a 4 × 2 × 4 Monkhorst–Pack grid; the total energy was converged to 5.0 × 10^{-6} eV per atom and the maximum forces between atoms were less than 0.01 eV $Å^{-1}$. The grid for the fast Fourier transform was 72 × 80 × 60.

4 Results and discussion

4.1 The THz absorption spectra of GABA

Fig. 2 shows the broadband THz absorption spectra of GABA and COC ranging from 0.5 to 18 THz at room temperature. GABA has a series of absorption peaks at 1.13, 1.52, 2.03, 2.58, 3.48, 4.34, 8.26 THz and five strong and sharp absorption peaks at 5.53, 7.80, 9.63, 12.0 and 16.7 THz respectively. The red line in the inset plot exhibits the THz absorption spectrum of GABA obtained by the TAS7400TS THz system ranging from 0.5 to 4.0 THz at room temperature. Except for some deviations of the absorption peak at about 1 THz, the absorption of the broadband spectrum below 4.0 THz obtained by the air-plasma THz system are precisely consistent with the red line in the inset plot. To figure out the spectral difference around 1 THz, an additional THz system based on the photoconductive switch was carried out whose effective range is 0.2 to 2.5 THz (see the black line in the inset plot). And the absorption peak around 1 THz of the spectrum agrees with the data from the TAS7400TS THz system. This is probably because the broadband air-plasma THz system has limitations at about 1 THz. It should be pointed out that the absorption peaks in the gray slash area after 17 THz are not very accurate and are for reference only, because this region may be beyond the effective detection range of the system. The broadband spectrum of GABA below 4.0 THz agrees well with the study of Peng *et al.*[21] As we can see in Fig. 2, COC was found to be suitable for THz spectroscopy applications for its negligible absorption below 13 THz, but there is obvious absorption in the region of 13 to 16 THz (see the gray area in Fig. 2). In consideration of the contribution of COC to the absorption, the FTIR was also carried out to investigate the absorption of GABA (see ESI Fig. S2†). The result shows that GABA has two main absorption peaks at 12.2 and 16.8 THz from 12 to 18 THz, which agrees with our observation of GABA by the broadband air-plasma THz system. And the result also shows that there is no obvious absorption between 13 and 16 THz. It suggests the reliability of the observation by our broadband air-plasma THz system. And the absorption of GABA between 13 and 16 THz in Fig. 2 (gray area) mainly comes from the COC. The experimental results indicate that GABA has rich resonance peaks in the THz band. The multiple verification of different THz systems shows that the broadband air-plasma THz system can provide more information about the vibrational properties

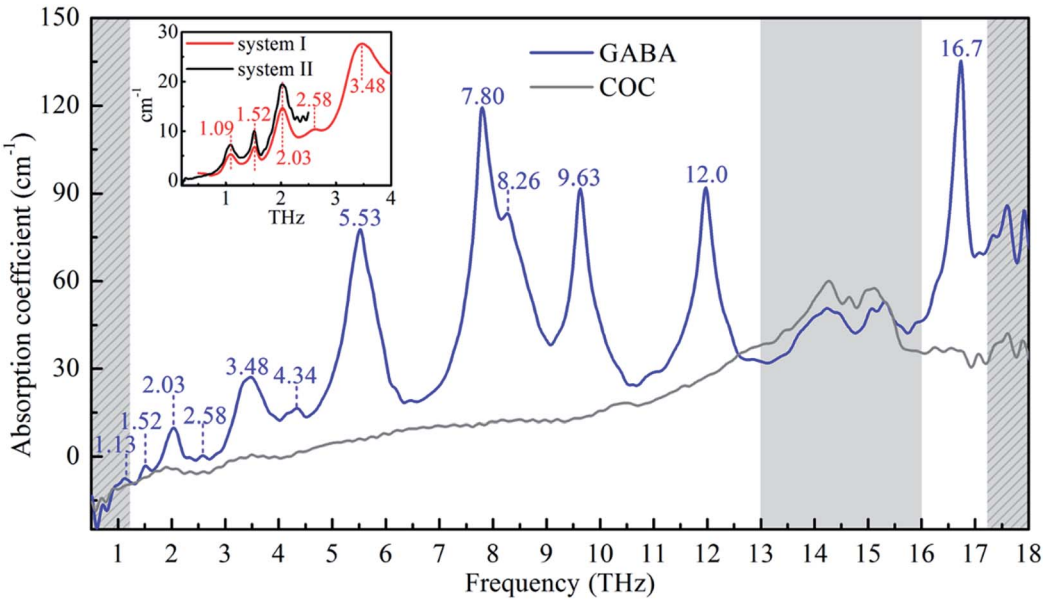

Fig. 2 The THz absorption spectra of GABA and COC obtained by the broadband air-plasma THz system at 293 K. The inset one was obtained by the TAS7400TS THz system (system I) and the photoconductive switch THz system (system II). (The gray area indicates that the contribution of substrate to the absorption. The absorption in the gray slash area is for reference only).

of material. These THz fingerprints of GABA can be utilized as biomarker in molecular detection and identification.

4.2 GABA quantum chemical calculations

Understanding the relationship between molecular vibration and structure as well as the physical mechanism of interaction in the THz spectrum is still a challenge at present. Quantum chemical calculations have been found to be an effective way to understand and interpret the experimental THz absorption properties.[28,29] Considering the experimental sample is a crystal powder, intermolecular interactions should be considered in the THz spectral analysis. Calculations based on the crystal cell have been suggested to be more reliable than those based on the isolated molecule.[30]

The calculated THz spectrum of GABA is plotted against the experimental one in Fig. 3. It can be seen that the experimental spectrum is roughly in agreement with the calculated one. The temperature difference is main reason of the spectral deviations between the two. The calculated spectrum was performed at 0 K while the experimental broadband THz spectrum in Fig. 3 was measured at 293 K. Meanwhile, the disparity of the crystals conditions in actual experiments and theoretical simulations also need to be taken into consideration.[11] The crystal cell parameters used for the calculations are derived from crystals recrystallized from aqueous solution.[8] However, the GABA used in our experiment was a commercially obtained powder crystal, and its crystalline quality was not as good as that of recrystallization from solution. In addition, the humidity and pressure are also the factors influencing the experiments.

In order to explain the deviations between the experimental and the calculated spectra, the variable temperature experiment was carried out. Fig. 4 shows the evolution of the THz spectra of GABA from 83 to 363 K. Thirty-six spectra were measured with the TAS7400TS fast-scanning THz system. As we can see in Fig. 4, the broad peak at 3.50 THz splits into shoulder peaks at 3.36 and 3.74 THz upon cooling. An unusual thermal behaviour that occurs at 1.13 THz at 363 K shifts to 0.79 THz at 83 K was exhibited in Fig. 4. The absorption peaks at 1.52, 2.03, and 2.63 THz, at 293 K, blue-shifted with decreasing temperature. All the absorption peaks become more distinct upon cooling. The results of variable temperature experiment agrees well with that of Dampf *et al.*[20] They attributed the unusual thermal behaviour to the distortion of a specific weak intermolecular hydrogen bond in solid GABA, and they explained the spectral features generally narrow and shift to higher frequencies in response to cooling as the crystallographic unit cell changes with temperature. Besides, the degree of shift in different peaks is not the same, this is probably due to different vibrational modes having different degrees of response to the temperature change. The difference between the experimental and calculated THz spectra of GABA is well explained by the variable temperature experiment.

4.3 Vibrational modes analysis

In order to describe the vibration of the GABA molecule in detail, the carbon atomic nomenclature of the GABA molecule in the lattice is depicted in Fig. 5a. To better comprehend the low-frequency vibration of GABA, the hydrogen bonds network of GABA lattices is shown in Fig. 5b.

Four typical vibrational modes of GABA (1.15, 1.39, 8.53, and 17.05 THz) are presented in Fig. 6. The experimental peaks at 1.09 and 1.52 THz correspond to the calculated modes at 1.15 and 1.39 THz, arising from rotation and translation of GABA, respectively, with all atoms involved. They indicate that at 1.09

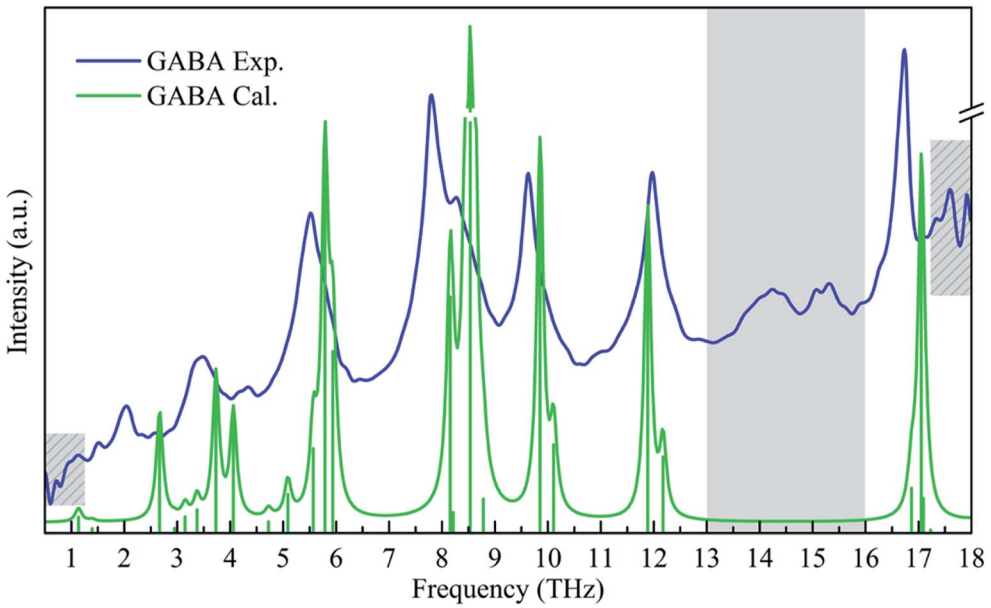

Fig. 3 Experimental and calculated spectra of GABA.

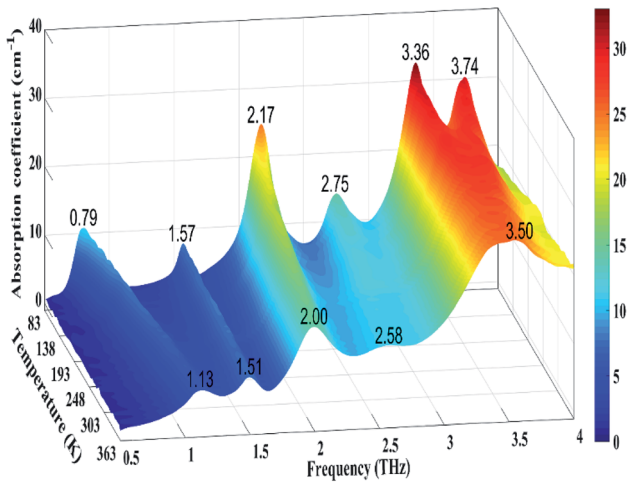

Fig. 4 Evolution of the THz spectra of GABA from 83 to 363 K (The color bar indicates the magnitude of the absorption coefficient).

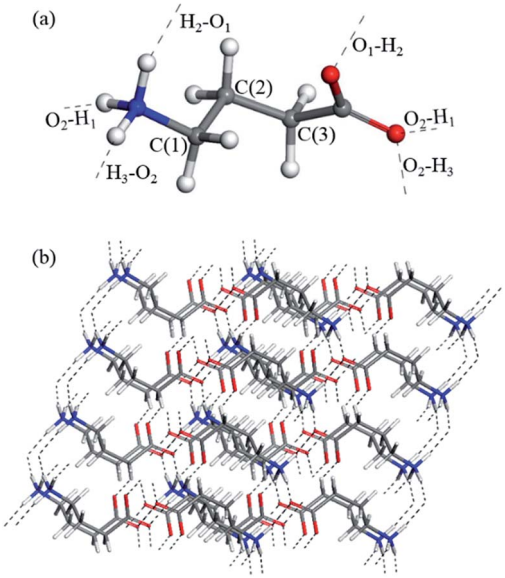

Fig. 5 (a) Carbon atomic nomenclature of the GABA molecule in the lattice, C(1) = C^{γ}, C(2) = C^{β}, C(3) = C^{α}. (b) The hydrogen bonds network (black dashed lines) of GABA lattices.

and 1.52 THz, the characteristic features of GABA come from distinct collective vibrations of the molecule or lattice mode. The broad 3.48 THz peak at 293 K, split into shoulder peaks at 83 K, which can be attributed to the calculated modes at 3.73 and 4.06 THz, comes from the $C^{\alpha}C^{\beta}C^{\gamma}N$ skeleton deformation, translation of the COO^{-} group at 3.73 THz and rocking of the COO^{-} group at 4.06 THz. In addition, the measured feature at 8.26 THz corresponds to the vibrational mode calculated at 8.53 THz, mainly from the wagging of the $C^{\alpha}C^{\beta}C^{\gamma}$ skeleton and rocking of the NH_3^{+} group. These results suggest that at higher THz frequencies, the absorptions also take along part of collective vibrations but mainly from the specific and local movements of the molecule. The descriptions of the calculated vibrational modes of GABA are shown in Table 1. By analyzing the vibrational modes of GABA between 0.5 and 18 THz, it was found that most of the vibrations are collective, but there were differences in the contribution of the skeleton and functional groups. Hand *et al.*[15] revealed that THz spectra of many biomolecules above 6 THz corresponding to available conformational states and dense transitions between phonon modes. As a functional group of GABA, amino is closely related to the biological effects of the molecule. Taking the amino group as an example, its motions after 5.80 THz make a more prominent contribution to the vibration of GABA. This may indicate the

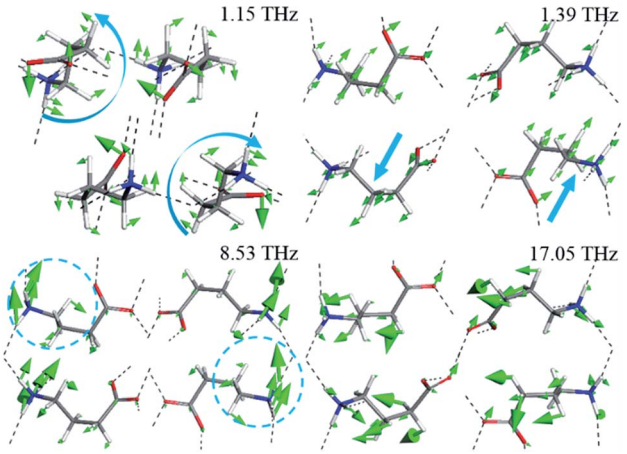

Fig. 6 Calculated vibrational modes of GABA at 1.15, 1.39, 8.53, and 17.05 THz (The blue arrows represent the direction of the molecular vibration).

Table 1 Comparison of the absorption peak positions between the experimental and calculated GABA spectra and vibrational modes assignment[a]

Exp./THz		Cal./THz	
293 K	83 K	0 K	Vibrational mode assignment
1.09	0.79	1.15	Collective
1.52	1.57	1.39	Collective
2.03	2.17	2.68	$t(COO^-) + \nu(C^\alpha C^\beta C^\gamma) + t(NH_3^+)$
2.58	2.75	3.16	Mainly from $r(C^\alpha C^\beta C^\gamma) + t(NH_3^+)$
		3.37	Mainly from $t(C^\alpha C^\beta C^\gamma)$
3.48	3.36	3.73	$t(COO^-) + \delta_{tw}(C^\alpha C^\beta C^\gamma N)$
	3.74	4.06	$r(COO^-) + \omega(C^\alpha C^\beta C^\gamma N)$
4.34		4.72	$r(COO^-) + \delta_{tw}(C^\alpha C^\beta C^\gamma N)$
		5.08	Mainly from $\nu(C^\beta C^\gamma)$
5.53		5.59	Mainly from $\nu(C^\beta C^\gamma)$
		5.80	Mainly from $r(C^\alpha C^\beta C^\gamma) + t(NH_3^+)$
		5.92	$r(COO^-) + r(C^\alpha C^\beta C^\gamma N)$
7.80		8.17	Mainly from $\delta(C^\alpha C^\beta C^\gamma) + r(NH_3^+)$
8.26		8.53	Mainly from $\omega(C^\alpha C^\beta C^\gamma) + r(NH_3^+)$
9.63		9.85	$r(COO^-) + \delta(C^\alpha C^\beta C^\gamma N)$
		10.09	$r(COO^-) + \delta(C^\alpha C^\beta C^\gamma N)$
12.0		11.89	$r(COO^-) + \delta(C^\alpha C^\beta C^\gamma) + r(NH_3^+)$
		12.16	$r(COO^-) + \delta(C^\alpha C^\beta C^\gamma) + r(NH_3^+)$
16.7		17.05	$t(COO^-) + \delta(C^\alpha C^\beta C^\gamma N)$

[a] ν, rotation; t, translation; ω, wagging; r, rocking; δ_{tw}, twisting; δ, bending.

structural or even conformational transformation of GABA molecule after 6 THz. Besides, although the frequencies of the absorption peaks at 8.17 and 8.53 THz are similar, their vibrational modes are quite different, which further indicates the complexity of the vibration of GABA in the THz band.

Chou[31] used a basic natural law to elucidate some important biological functions of an IgG antibody molecule. He suggested that when the dominant low-frequency amplitude of a domain is larger, the energy barrier which must be surmounted for a successful biochemical reaction is more easily overcome.[32] Consequently, the variation of the dominant low-frequency amplitudes of various domains in an antibody molecule will reflect not only the effects of physical coupling but, more importantly, their mutual influence in the biological function.[30] Recently, Woods *et al.*[33] found that during the photo-isomerization process, the retinal low-frequency motion is directly tied with the overall protein configuration. Balu *et al.*[34] demonstrated that low-frequency vibrations are related to the conformational changes in bacteriorhodopsin and rhodopsin. GABA ligand can interact with diverse receptors. The resonant coupling at different frequencies corresponds to the specific molecular structures and interactions. The structural fluctuations of the flexible ligand play a critical role in the conformational selection in proteins. GABA functions appear to be triggered by binding of GABA to its ionotropic and metabotropic receptors, and the diversity in the pharmacologic properties of the receptor subtypes is clinically important.[35] Structural or conformational fluctuations and microenvironment changes of the neurotransmitter may affect the mutual recognition and interactions between the ligand and the receptors, which have potential impact on biological events such as specific selection, signal transmission, and activation of biomolecules. Therefore, the properties of the low-frequency vibrational modes in a wide THz region provide useful information for understanding the neurotransmitter molecule and may also throw some light on the biological function of GABA in the synapse.

5 Conclusions

The broadband THz spectrum of GABA was investigated with an air-plasma THz system from 0.5 to 18 THz and distinct absorption peaks were obtained. Two additional THz systems and FTIR were also used in different regions to verify the GABA absorptions. The results demonstrated that the broadband air-plasma THz system is reliable and that the THz fingerprints of GABA can be used as biomarkers in molecular detection and identification. The difference between the experimental and the calculated spectra was well explained by the variable temperature experiment. The DFT calculation based on the crystal cell was performed and the results showed that at 1.15 and 1.39 THz, the characteristic absorption peaks of GABA come from distinct collective vibrations. At higher THz frequencies, the characteristic features come mainly from the specific and local vibration of the molecule, which can reflect the characteristics of the microenvironment. In addition, the change of the amino group vibration after 6 THz may indicate the structural or even conformational transformation of GABA molecule. These is crucial for understanding, at the molecular level, the biological function of this significant neurotransmitter.

Conflicts of interest

There are no conflicts to declare.

Acknowledgements

This work was supported by the Main Direction Program of Knowledge Innovation and Open Project Program of Key Laboratory of Interfacial Physics and Technology, Chinese Academy of Sciences (No. Y627041011), the National Natural Science Foundation of China (Grants No. 51677145) and the National Defense Science and Technology Innovation Special Zone.

References

1 D. Majumdar and S. Guha, Conformation, electrostatic potential and pharmacophoric pattern of GABA (gamma-aminobutyric acid) and several GABA inhibitors, *J. Mol. Struct.: THEOCHEM*, 1988, **180**, 125–140.

2 C. M. da Silva, J. G. Silva, G. S. Pinheiro, R. C. Vilela, F. E. A. Melo, J. A. Lima and P. T. C. Freire, Raman spectroscopy of gamma-aminobutyric acid under high pressure, *Vib. Spectrosc.*, 2017, **92**, 162–168.

3 G. A. R. Johnston, GABA(A) receptor channel pharmacology, *Curr. Pharm. Des.*, 2005, **11**, 1867–1885.

4 S. T. Zhu, C. M. Noviello, J. F. Teng, R. M. Walsh, J. J. Kim and R. E. Hibbs, Structure of a human synaptic GABA(A) receptor, *Nature*, 2018, **559**, 67–72.

5 J. Strom, J. Them, F. Mansson, J. Ahl, T. C. Savidge, S. M. Dann and F. Resman, The association between GABA-modulators and clostridium difficile infection - a matched retrospective case-control study, *PLoS One*, 2017, **12**, 1–12.

6 O. A. C. Petroff, GABA and glutamate in the human brain, *Neuroscientist*, 2002, **8**, 562–573.

7 E. G. Steward, R. B. Player and D. Warner, Crystal and molecular-structure of gamma-aminobutyric acid determined at low-temperature, *Acta Crystallogr., Sect. B: Struct. Sci.*, 1973, **29**, 2038–2045.

8 H. P. Weber, B. M. Craven and R. K. Mcmullan, The neutron structure of and thermal motion in gamma-aminobutyric acid (GABA) at 122 K, *Acta Crystallogr., Sect. B: Struct. Sci.*, 1983, **39**, 360–366.

9 A. J. Dobson and R. E. Gerkin, Gamma-aminobutyric acid: a novel tetragonal phase, *Acta Crystallogr., Sect. C: Cryst. Struct. Commun.*, 1996, **52**, 3075–3078.

10 M. M. Naffaa, S. Hung, M. Chebib, G. A. R. Johnston and J. R. Hanrahan, GABA- receptors: distinctive functions and molecular pharmacology, *Br. J. Pharmacol.*, 2017, **174**, 1881–1894.

11 T. T. Pan, S. P. Li, T. Zou, Z. Yu, B. Zhang, C. Y. Wang, J. B. Zhang, M. X. He and H. W. Zhao, Terahertz spectra of l-phenylalanine and its monohydrate, *Spectrochim. Acta, Part A*, 2017, **178**, 19–23.

12 L. Ho, M. Pepper and P. Taday, Terahertz spectroscopy: signatures and fingerprints, *Nat. Photonics*, 2008, **2**, 541–543.

13 T. Sasaki, T. Sakamoto and M. Otsuka, Detection of impurities in organic crystals by high-accuracy terahertz absorption spectroscopy, *Anal. Chem.*, 2018, **90**, 1677–1682.

14 A. Markelz, S. Whitmire, J. Hillebrecht and R. Birge, THz time domain spectroscopy of biomolecular conformational modes, *Phys. Med. Biol.*, 2002, **47**, 3797–3805.

15 K. Hand and E. Yates, Terahertz: dictating the frequency of life. Do macromolecular vibrational modes impose thermal limitations on terrestrial life?, *J. R. Soc., Interface*, 2017, **14**, 20170673.

16 N. Karpowicz, J. M. Dai, X. F. Lu, Y. Q. Chen, M. Yamaguchi, H. W. Zhao, X. C. Zhang, L. L. Zhang, C. L. Zhang, M. Price-Gallagher, C. Fletcher, O. Mamer, A. Lesimple and K. Johnson, Coherent heterodyne time-domain spectrometry covering the entire "terahertz gap", *Appl. Phys. Lett.*, 2008, **92**, 01131.

17 T. Bartel, P. Gaal, K. Reimann, M. Woerner and T. Elsaesser, Generation of single-cycle THz transients with high electric-field amplitudes, *Opt. Lett.*, 2005, **30**, 2805–2807.

18 J. Dai, X. Xie and X. C. Zhang, Detection of broadband terahertz waves with a laser-induced plasma in gases, *Phys. Rev. Lett.*, 2006, **97**, 103903.

19 A. G. Markelz, Terahertz dielectric sensitivity to biomolecular structure and function, *IEEE J. Sel. Top. Quantum Electron.*, 2008, **14**, 180–190.

20 S. J. Dampf and T. M. Korter, Anomalous temperature dependence of the lowest-frequency lattice vibration in crystalline gamma-aminobutyric acid, *J. Phys. Chem. A*, 2019, **123**, 2058–2064.

21 Y. Du, J. D. Xue, Q. Cai and Q. Zhang, Spectroscopic investigation on structure and pH dependent cocrystal formation between gamma-aminobutyric acid and benzoic acid, *Spectrochim. Acta, Part A*, 2018, **191**, 377–381.

22 Y. Peng, X. R. Yuan, X. Zou, W. Q. Chen, H. Huang, H. W. Zhao, B. Song, L. Chen and Y. M. Zhu, Terahertz identification and quantification of neurotransmitter and neurotrophy mixture, *Biomed. Opt. Express*, 2016, **7**, 4472–4479.

23 F. D'Angelo, Z. Mics, M. Bonn and D. Turchinovich, Ultra-broadband THz time-domain spectroscopy of common polymers using THz air photonics, *Opt. Express*, 2014, **22**, 12475–12485.

24 K. Tomita, H. Higashi and T. Fujiwara, Crystal and molecular-structure of omega-amino acids, omega-amino sulfonic acids and their derivatives 4. The crystal and molecular-structure of gamma-aminobutyric acid (GABA), a nervous inhibitory transmitter, *Bull. Chem. Soc. Jpn.*, 1973, **46**, 2199–2204.

25 B. M. Craven and H. P. Weber, Charge-density in the crystal-structure of gamma-aminobutyric acid at 122 K - an intramolecular methylene H-bridge, *Acta Crystallogr., Sect. B: Struct. Sci.*, 1983, **39**, 743–748.

26 S. J. Clark, M. D. Segall, C. J. Pickard, P. J. Hasnip, M. J. Probert, K. Refson and M. C. Payne, First principles methods using CASTEP, *Z. Kristallogr.*, 2005, **220**, 567–570.

27 J. P. Perdew, K. Burke and M. Ernzerhof, Generalized gradient approximation made simple, *Phys. Rev. Lett.*, 1996, **77**, 3865–3868.

28 D. F. Plusquellic, K. Siegrist, E. J. Heilweil and O. Esenturk, Applications of terahertz spectroscopy in biosystems, *ChemPhysChem*, 2007, **8**, 2412–2431.

29 F. Zhang, H. W. Wang, K. Tominaga, M. Hayashi, T. Hasunuma and A. Kondo, Application of THz

vibrational spectroscopy to molecular characterization and the theoretical fundamentals: an illustration using saccharide molecules, *Chem.–Asian J.*, 2017, **12**, 324–331.

30 T. R. Juliano and T. M. Korter, Terahertz vibrations of crystalline acyclic and cyclic diglycine: benchmarks for london force correction models, *J. Phys. Chem. A*, 2013, **117**, 10504–10512.

31 K. C. Chou, The biological functions of low-frequency vibrations (phonons) 6. A possible dynamic mechanism of allosteric transition in antibody molecules, *Biopolymers*, 1987, **26**, 285–295.

32 K. C. Chou, Low-frequency collective motion in biomacromolecules and its biological functions, *Biophys. Chem.*, 1988, **30**, 3–48.

33 K. N. Woods, J. Pfeffer, A. Dutta and J. Klein-Seetharaman, Vibrational resonance, allostery, and activation in rhodopsin-like G protein-coupled receptors, *Sci. Rep.*, 2016, **6**, 37290.

34 R. Balu, H. Zhang, E. Zukowski, J. Y. Chen, A. G. Markelz and S. K. Gregurick, Terahertz spectroscopy of bacteriorhodopsin and rhodopsin: similarities and differences, *Biophys. J.*, 2008, **94**, 3217–3226.

35 M. Watanabe, K. Maemura, K. Kanbara, T. Tamayama and H. Hayasaki, GABA and GABA receptors in the central nervous system and other organs, *Int. Rev. Cytol.*, 2002, **213**, 1–47.